Eur. Phys. J. D **6**, 1–7 (1999)

THE EUROPEAN PHYSICAL JOURNAL D

EDP Sciences

Atomic lifetimes and transition probabilities in boron-like (Na VII) and beryllium-like (Na VIII) sodium ions

X. Tordoir[1], E. Biémont[1,2,a], H.P. Garnir[1], P.-D. Dumont[1], and E. Träbert[3]

[1] Institut de Physique Nucléaire Expérimentale, Université de Liège B15, Sart Tilman, 4000 Liège, Belgium
[2] Astrophysique et Spectroscopie, Université de Mons-Hainaut, 7000 Mons, Belgium
[3] Experimentalphysik III, Ruhr-Universität Bochum, 44780 Bochum, Germany

Received: 18 November 1998

Abstract. Spectra and decay curves of boron-like (Na VII) and beryllium-like (Na VIII) sodium ions produced by beam-foil excitation have been recorded in the 30–60 nm spectral range and the radiative lifetimes of seven $n = 2$ levels have been measured. The experimental results are compared with the available theoretical values and with new results obtained in the framework of two theoretical approaches: the Relativistic Hartree-Fock approximation and the Multiconfiguration Dirac-Fock method. Corroborated by the fair agreement of the new theory data with experiment, a new set of accurate transition probabilities for the $2s^2 2p$-$2s2p^2$ and $2s2p^2$-$2p^3$ transitions of Na VII is presented.

PACS. 32.70.-n Intensities and shapes of atomic spectral lines

1 Introduction

The spectrum of Na VII is still rather poorly known, particularly for the highly excited levels. The compilation of the energy levels by Martin and Zalubas [1] is essentially based on the analyses by Söderqvist [2,3]. Additional information has been provided by Fawcett [4] and by Edlén [5]. As emphasized in reference [1], several levels are listed as questionable because they have been obtained from the consideration of weak lines. In addition, due to the interaction with configurations based on different cores, the interpretation of some of the higher levels should probably be regarded as tentative. The position of the quartet system is not yet accurately established, because no definite data on quartet-doublet transitions are available. Most of the wavelengths quoted by Kelly [6] are taken from the analyses by Söderqvist [2,3].

The experimental determination of transition probabilities or lifetimes in Na VII is extremely fragmentary. To our knowledge, the only work has been published by Buchet *et al.* [7] twenty years ago and only one lifetime (for $2s2p^2\ ^2P$) has been reported in their paper. This lack of experimental investigations is mainly due to the difficulty of not having an ion source that is able to produce a sufficiently intense and steady sodium beam. In contrast, Si is easily available as an intense ion beam, facilitating a thorough study [8–10].

Several theoretical investigations of transition probabilities and oscillator strengths have been published on Na VII. The "old" NBS compilation [11] was essentially based on calculations of Cohen and Dalgarno [12] which included limited configuration mixing. Consequently, the uncertainties quoted in reference [11] were estimated to be typically within 50 percent. Additional information, mainly for the $2p\ ^2P^o$-$3s\ ^2S$ and $2p\ ^2P^o$-$3d\ ^2D$ multiplets, was obtained by exploiting the dependence of f-values on nuclear charge and by using graphical interpolation. The boron isoelectronic sequence has been considered by Weiss [13] (SOC method) who computed f-values for transitions between a number of low-lying levels in B I and Ne VI and who used a graphical study of the f-value behaviour along the isoelectronic sequence to deduce results in Na VII. Radiative and collisional atomic data have been obtained by Flower and Nussbaumer [14] for transitions within the $2s^2 2p$, $2s2p^2$ and $2p^3$ configurations of Na VII, Si X and S XII, some of them being of interest for the interpretation of coronal observations. Using a simple Multi-Configuration Hartree-Fock approach (MCHF) with Breit-Pauli corrections included, Dankwort and Trefftz [15] calculated oscillator strengths (2-2 and 2-3 transitions) in some highly ionized boron-like ions up to Fe XXII. Although they did not consider specifically the Na VII case, numerical values for this ion can be deduced from interpolation in their tables. E1 2-2 transitions in the boron isoelectronic sequence have been considered by Fawcett [16] who performed HXR calculations using a version of the Cowan code [17,18] as developed by Bromage [19]. The work by Farrag *et al.* [20,21] concerning the boron sequence, although not focussing on the Na VII ion, shows graphical representations of trends of f-values along the sequence for the $n = 2$-2 transitions.

[a] e-mail: e.biemont@ulg.ac.be

A frozen-core Hartree-Fock procedure incorporating an l-dependent core polarization potential was considered by McEachran and Cohen [22] for the $2p$-$3s$, $2p$-$3d$, $3s$-$3p$ and $3p$-$3d$ transition arrays along the boron sequence up to Na VII. The quantum defect orbital formalism (QDO) has been applied by Lavin and Martin [23] to the calculation of f-values for the $1s^2 2s^2 np\ ^2P^\circ$ - $1s^2 2s^2 ms\ ^2S$ (n = 2-3, m = 3-4) transitions. In the framework of the Opacity Project, close-coupling calculations have been performed along the boron isoelectronic sequence ($n \leq 10$) by Luo and Pradhan [24] using the R-matrix method. The results reported [25], however, are obtained in LS coupling and do not take fine structure into account. Finally, using MCDF wave functions calculated with Grant's code [26–28], the n = 2-2 transitions along the boron sequence have been considered by Zhang and Sampson [29].

The beryllium-like ions, and more particularly Na VIII, have been the subject of many theoretical studies (for the relevant references, see the different NIST compilations) but no experimental lifetimes are available for that ion. The only experimental work is due to Granzow *et al.* [30] who considered the transition probabilities of the $1s^2 2s^2\ ^1S_0$ - $1s^2 2s3p\ ^3P_1^\circ$ intercombination line in Be-like ions of Na through Si.

In view of this lack of experimental data, we have performed here lifetime measurements in Na VII and Na VIII for 7 levels belonging to the $2s2p^2$, $2p^3$ and $2s2p$ configurations, respectively. The comparison of these experimental results with new f-values obtained in the framework of the HFR and MCDF techniques allows to assess the reliability of the theory and to obtain a new set of accurate transition probabilities for the n = 2-2 transitions of Na VII.

2 Experiment

The experiment was carried out using the Dynamitron Tandem accelerator at Bochum University. Negatively charged sodium ions were produced in a Middleton-type heavy-ion sputter source loaded with a cylindrical cathode (pressed from a powder) that contained mostly Na_2CO_3 and a fraction of Ag. This material is somewhat hygroscopic and its surface suffers from exposure to air. Therefore the cathodes need to be prepared freshly, but they then last in the ion source (under vacuum) for about a day. This preparation and handling seems to be easier and yields a more reliable and steady ion beam than Middleton's original recipe of using NaOH or NaCl. An Na^- ion beam of about 1.3 μA was extracted from the source, and typically a particle current of up to 0.15 μA (in charge state $q = +2$) was directed to the target chamber and collected in a Faraday cup placed behind the foil. Carbon foils with an areal density of about 10 μg/cm^2 were used throughout the experiment.

The beam-foil induced light was observed at right angle of the ion beam with a grazing incidence monochromator (McPherson Mod. 247, R = 2.2 m) equipped with a ruled 600 lines/mm concave grating and a channeltron detector of very low dark count rate (< 1 count/min). A spectral resolution of 60 pm (FWHM) was obtained with 80 μm slits. Narrower slits were used for detailed spectra. The spectrometer was calibrated from known lines [6] which are observed in the spectra.

Sodium spectra in the wavelength range 12 to 55 nm were recorded at several ion energies (1.5, 3.0, 4.5 and 7.0 MeV). The lines of Na VII were the most intense in the 7 MeV spectrum and, consequently, this energy was chosen for most of the lifetime measurements; only one lifetime (for $2s2p^2\ ^2S$) was measured at both 4.5 and 7.0 MeV. Figure 1 shows the spectrum obtained and the most intense transitions identified as being due to Na VII. The photon counting rates have been normalized to equal amounts of integrated beam charge measured in the Faraday cup. For the lifetime measurements, the light intensity of a selected line was recorded as a function of the displacement of the excitation foil along the beam axis in front of the entrance slit of the spectrometer. The positioning of the foil was achieved with a step motor and a precision lead screw the linearity of which had been checked using a Heidenhain moire fringe length gauge reading to within 1μm.

3 Calculations

Two different theoretical methods were considered in the present paper. The first one is the fully relativistic multiconfiguration Dirac-Fock approximation (MCDF) developed by Grant and coworkers [26–28]. The calculation was completed with the inclusion of the relativistic two-body Breit interaction and of the quantum electrodynamical corrections (QED) due to self-energy (SE) and vacuum polarization (VP). The extended average level optimization (EAL) process was used for performing the calculation of the energy levels and transition probabilities. 17 non-relativistic configurations were considered in Na VII which are supposed to account for the largest part of the configuration interaction effects. They are: $1s^2 2p^3 + 1s^2 2s^2 2p + 1s^2 2s^2 3p + 1s^2 2s2p3s + 1s^2 2s2p3d + 1s2s^2 2p3s + 1s2s^2 2p3d + 1s^2 2p^2 3p$ and $1s^2 2s2p^2 + 1s2p^4 + 1s2s^2 2p^2 + 1s2s^2 2p3p + 1s^2 2s^2 3s + 1s^2 2s^2 3d + 1s^2 2s2p3p + 1s^2 2p^2 3s + 1s^2 2p^2 3d$. In Na VIII, the following 19 configurations were retained: $1s^2 2s^2 + 1s^2 2p^2 + 1s^2 2s3s + 1s^2 2s3d + 1s2s^2 3s + 1s2s^2 3d + 1s^2 2p3p + 1s^2 3s^2 + 1s^2 3p^2 + 1s^2 3d^2$ and $1s^2 2s2p + 1s2p^3 + 1s2s^2 2p + 1s2s^2 3p + 1s^2 2s3p + 1s^2 2p3s + 1s^2 2p3d + 1s^2 3s3p + 1s^2 3p3d$.

The second method is a pseudo-relativistic Hartree-Fock (HFR) technique [17,18]. Although based on the (non-relativistic) Schrödinger equation, the HFR method does consider the most important relativistic effects via added interactions. In that approach, the average energies, the Slater integrals and the spin-orbit integrals are first calculated *ab initio* and afterwards eventually adjusted through comparison of the calculated eigenvalues of the Hamiltonian with observed energy levels, so that discrepancies between computed and measured energy levels are minimized. For many different ions, this HFR approach has been able to provide a fair agreement with measurements performed using laser excitation (see, *e.g.*, references [31–34]). In view of the uncertainties affecting many

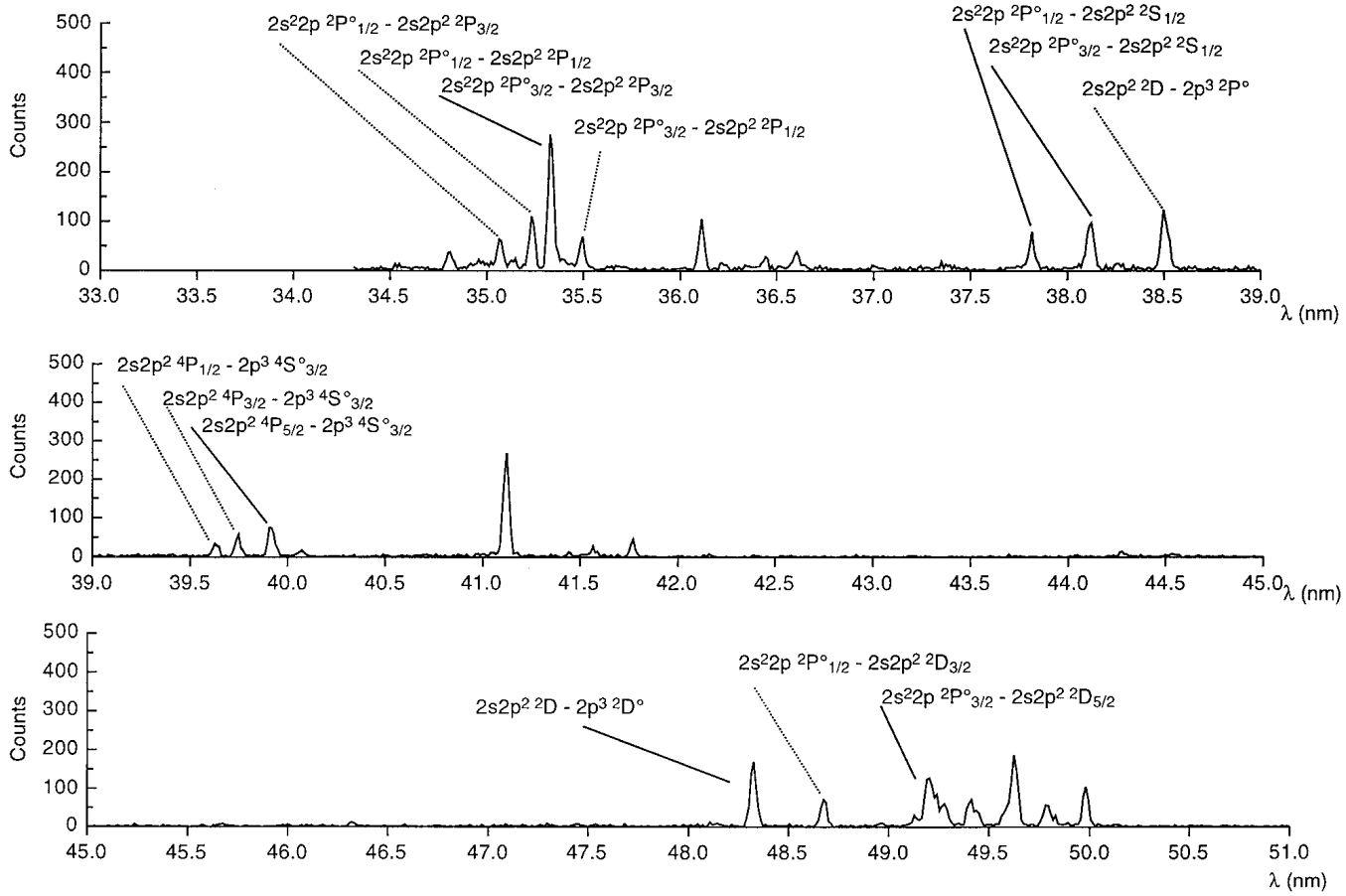

Fig. 1. Sample of the spectrum as it was observed between 33 and 51 nm. The identified transitions are indicated in the figure.

energy levels determined experimentally in Na VII, particularly those belonging to the $n \geq 3$ configurations, we have preferred not to use the least-squares optimization routine in the present work but to extend as much as possible the number of configurations explicitly introduced in the physical model adopted. The 45 configurations retained for the calculations are: $1s^22s^2np(n = 2\text{-}5) + 1s^22s^2nf(n = 4\text{-}5) + 1s^22p^3 + 1s^22p^2np(n = 3\text{-}5) + 1s^22s2pns(n = 3\text{-}5) + 1s^22s2pnd(n = 3\text{-}5) + 1s2s^22pns(n = 3\text{-}5) + 1s2s^22pnd(n = 3\text{-}5)$ and $1s^22s2p^2 + 1s^22s^2ns(n = 3\text{-}5) + 1s^22s^2nd(n = 3\text{-}5) + 1s^22s2pnp(n = 3\text{-}5) + 1s^22s2pnf(n = 4\text{-}5) + 1s2s^22p^2 + 1s2s^22pnp(n = 3\text{-}5) + 1s^22p^2ns(n = 3\text{-}5) + 1s^22p^2nd(n = 3\text{-}5) + 1s2p^4$. In Na VIII, the following 52 configurations were considered: $1s^22s^2 + 1s^22sns(n = 3\text{-}5) + 1s^22snd(n = 3\text{-}5) + 1s2s^2ns(n = 3\text{-}5) + 1s2s^2nd(n = 3\text{-}5) + 1s2s2pnp(n = 3\text{-}5) + 1s2s2pnf(n = 4\text{-}5)$ and $1s^22snp(n = 2\text{-}5) + 1s^22snf(n = 4\text{-}5) + 1s2s^2np(n = 2\text{-}5) + 1s2s^2nf(n = 4\text{-}5) + 1s2s2pns(n = 3\text{-}5) + 1s^22pns(n = 3\text{-}5) + 1s^22pnd(n = 3\text{-}5) + 1s2p^3$.

The lifetime values as obtained in the present work by using both the MCDF and the HFR methods are reported in Table 1 (columns 3 and 4) for Na VII and Na VIII. Both sets of results are in close agreement with each other and they agree also well with the experimental data (column 2). In fact, in Na VII, the mean ratios $\tau_{\rm EXP}/\tau_{\rm HFR}$ and $\tau_{\rm EXP}/\tau_{\rm MCDF}$ are 1.010 ± 0.095 and 1.044 ± 0.052 where the quoted uncertainties correspond to the standard deviation. In Na VIII, the same ratios are equal to 0.917 and 1.019, respectively.

The HFR and MCDF (Babushkin gauge) f-values calculated in an *ab initio* way for the $2s^22p$-$2s2p^2$ and $2s2p^2$-$2p^3$ transitions of Na VII are given in Table 2. It is seen that both sets of results are generally in excellent agreement not only for the strong $\Delta S = 0$ transitions but also for the very weak intercombination lines for which accurate calculations are generally more difficult. In view of the fact that these two sets of independent results agree very well with each other and that the deduced lifetimes agree well with experiment, the new f-values are expected to be very accurate.

4 Experimental results

A partial Grotrian diagram showing the low excitation levels of Na VII is shown in Figure 2. The $n = 2$ configurations ($2s^22p$, $2s2p^2$ and $2p^3$) give rise to 6 multiplets in the doublet system and to 2 multiplets in the quartet system. A few observed wavelengths [6] are indicated in the figure. With the exception of the $2p^3\ ^2P^\circ$ term not measured in the present work, lifetime measurements of

all $n = 2$ terms in boron-like sodium have been deduced from the analysis of the relevant beam-foil decay curves. In Figure 3, we present a typical decay curve ($2p^3\ ^2D^\circ_{5/2}$ level) which has been fitted with a sum of two decaying exponentials convoluted with a Gaussian shaped observation window. Alternatively, a trapezoidal window shape, as suggested by experiment [9], was used, and up to 3 exponentials were employed in order to represent the primary decay and approximate the cascades. The strongest of these cascades into the first $n = 2$ levels (displaced terms) are those from the next higher group of displaced levels in the same shell. The speed of the ions was assumed to be 7.58 mm/ns. All our lifetime measurements as well as the previous measurement of reference [7] are summarized in Table 1.

5 Discussion of the results

5.1 General considerations

Ions with three electrons in the outer shell of the ground configuration (B sequence, Al sequence, ...) share a

Table 1. Na VII and Na VIII measured and calculated lifetimes.

Level	Lifetime(ns)			
	Theory (this work)			Previous work
	EXP.	HFR	MCDF	
Na VII				
$2p^3\ ^2P^\circ_{1/2,3/2}$		0.107	0.105	0.109[d], 0.112[f], 0.097[g]
$2p^3\ ^2D^\circ_{5/2}$	0.28 ± 0.04	0.244	0.271	0.247[d], 0.278[f], 0.239[g]
$2p^3\ ^2D^\circ_{3/2}$		0.245	0.272	0.275[d], 0.268[g]
$2p^3\ ^4S^\circ_{3/2}$	0.095 ± 0.010	0.087	0.088	0.092[a], 0.084[c], 0.085[d], 0.090[f], 0.083[g]
$2s2p^2\ ^2S_{1/2}$	0.155 ± 0.010	0.164	0.143	0.164[a], 0.164[b], 0.141[c], 0.159[d], 0.162[e], 0.162[f], 0.138[g]
$2s2p^2\ ^2P_{1/2}$	0.073 ± 0.010	0.083	0.077	0.748[a], 0.083[b], 0.082[c], 0.075[d], 0.083[e]
	0.076 ± 0.008[h]			0.083[f], 0.078[g]
$2s2p^2\ ^2D_{3/2}$	0.69 ± 0.05	0.665	0.659	0.732[a], 0.769[b], 0.645[c], 0.582[d], 0.737[e], 0.743[f], 0.623[g]
$2s2p^2\ ^2D_{5/2}$	0.70 ± 0.07	0.685	0.680	0.732[a], 0.769[b], 0.667[c], 0.600[d], 0.741[e], 0.743[f], 0.645[g]
Na VIII				
$2s2p\ ^1P^\circ_1$	0.21 ± 0.01	0.229	0.206	

[a] Reference [13]; [b] Reference [42]; [c] Reference [14]; [d] Reference [16]; [e] Reference [15]; [f] Reference [24]; [g]: Reference [29]; [h] Reference [7];
HFR : This work (HFR method);
MCDF : This work (MCDF approach - Babushkin gauge).

Table 2. Oscillator strengths for the n = 2-2 transitions of Na VII.

Transition	$\log gf$	
	HFR	MCDF
$2s^22p\ ^2P^\circ_{1/2}$-$2s2p^2\ ^4P_{1/2}$	−5.02	−5.23
$2s^22p\ ^2P^\circ_{1/2}$-$2s2p^2\ ^4P_{3/2}$	−6.35	−6.55
$2s^22p\ ^2P^\circ_{3/2}$-$2s2p^2\ ^4P_{1/2}$	−5.08	−5.25
$2s^22p\ ^2P^\circ_{3/2}$-$2s2p^2\ ^4P_{3/2}$	−5.31	−5.64
$2s^22p\ ^2P^\circ_{3/2}$-$2s^2p^2\ ^4P_{5/2}$	−4.67	−4.88
$2s^22p\ ^2P^\circ_{1/2}$-$2s2p^2\ ^2D_{3/2}$	−0.74	−0.76
$2s^22p\ ^2P^\circ_{3/2}$-$2s2p^2\ ^2D_{3/2}$	−1.49	−1.50
$2s^22p\ ^2P^\circ_{3/2}$-$2s2p^2\ ^2D_{5/2}$	−0.50	−0.52
$2s^22p\ ^2P^\circ_{1/2}$-$2s2p^2\ ^2S_{1/2}$	−0.95	−0.95
$2s^22p\ ^2P^\circ_{3/2}$-$2s2p^2\ ^2S_{1/2}$	−0.79	−0.76
$2s^22p\ ^2P^\circ_{1/2}$-$2s2p^2\ ^2P_{1/2}$	−0.54	−0.55
$2s^22p\ ^2P^\circ_{1/2}$-$2s2p^2\ ^2P_{3/2}$	−0.82	−0.83
$2s^22p\ ^2P^\circ_{3/2}$-$2s2p^2\ ^2P_{1/2}$	−0.76	−0.78
$2s^22p\ ^2P^\circ_{3/2}$-$2s2p^2\ ^2P_{3/2}$	−0.11	−0.12
$2s2p^2\ ^4P_{1/2}$-$2p^3\ ^4S^\circ_{3/2}$	−0.74	−0.76
$2s2p^2\ ^4P_{3/2}$-$2p^3\ ^4S^\circ_{3/2}$	−0.44	−0.46
$2s2p^2\ ^4P_{5/2}$-$2p^3\ ^4S^\circ_{3/2}$	−0.27	−0.28
$2s2p^2\ ^4P_{1/2}$-$2p^3\ ^2D^\circ_{3/2}$	−5.79	−5.91
$2s2p^2\ ^4P_{3/2}$-$2p^3\ ^2D^\circ_{5/2}$	−5.45	−5.49
$2s2p^2\ ^4P_{3/2}$-$2p^3\ ^2D^\circ_{3/2}$	−4.61	−4.68
$2s2p^2\ ^4P_{5/2}$-$2p^3\ ^2D^\circ_{5/2}$	−3.94	−4.00
$2s2p^2\ ^4P_{5/2}$-$2p^3\ ^2D^\circ_{3/2}$	−5.24	−5.40
$2s2p^2\ ^4P_{1/2}$-$2p^3\ ^2P^\circ_{1/2}$	−5.14	−5.18
$2s2p^2\ ^4P_{1/2}$-$2p^3\ ^2P^\circ_{3/2}$	−6.33	−7.73
$2s2p^2\ ^4P_{3/2}$-$2p^3\ ^2P^\circ_{1/2}$	−5.82	−5.98
$2s2p^2\ ^4P_{3/2}$-$2p^3\ ^2P^\circ_{3/2}$	−4.48	−4.60
$2s2p^2\ ^4P_{5/2}$-$2p^3\ ^2P^\circ_{3/2}$	−4.84	−5.06
$2s2p^2\ ^2D_{5/2}$-$2p^3\ ^4S^\circ_{3/2}$	−6.16	−6.36
$2s2p^2\ ^2D_{3/2}$-$2p^3\ ^4S^\circ_{3/2}$	−8.45	−7.70
$2s2p^2\ ^2D_{5/2}$-$2p^3\ ^2D^\circ_{5/2}$	−0.22	−0.24
$2s2p^2\ ^2D_{5/2}$-$2p^3\ ^2D^\circ_{3/2}$	−1.29	−1.32
$2s2p^2\ ^2D_{3/2}$-$2p^3\ ^2D^\circ_{5/2}$	−1.32	−1.35
$2s2p^2\ ^2D_{3/2}$-$2p^3\ ^2D^\circ_{3/2}$	−0.42	−0.44
$2s2p^2\ ^2D_{5/2}$-$2p^3\ ^2P^\circ_{3/2}$	−0.39	−0.38
$2s2p^2\ ^2D_{3/2}$-$2p^3\ ^2P^\circ_{1/2}$	−0.63	−0.62
$2s2p^2\ ^2D_{3/2}$-$2p^3\ ^2P^\circ_{3/2}$	−1.29	−1.29
$2s2p^2\ ^2S_{1/2}$-$2p^3\ ^4S^\circ_{3/2}$	−6.28	−6.90
$2s2p^2\ ^2S_{1/2}$-$2p^3\ ^2D^\circ_{3/2}$	−2.77	−2.97
$2s2p^2\ ^2S_{1/2}$-$2p^3\ ^2P^\circ_{1/2}$	−1.25	−1.28
$2s2p^2\ ^2S_{1/2}$-$2p^3\ ^2P^\circ_{3/2}$	−0.82	−0.86
$2s2p^2\ ^2P_{1/2}$-$2p^3\ ^4S^\circ_{3/2}$	−5.11	−5.33
$2s2p^2\ ^2P_{3/2}$-$2p^3\ ^4S^\circ_{3/2}$	−4.46	−4.75
$2s2p^2\ ^2P_{1/2}$-$2p^3\ ^2D^\circ_{3/2}$	−0.63	−0.68
$2s2p^2\ ^2P_{3/2}$-$2p^3\ ^2D^\circ_{5/2}$	−0.40	−0.45
$2s2p^2\ ^2P_{3/2}$-$2p^3\ ^2D^\circ_{3/2}$	−1.40	−1.44
$2s2p^2\ ^2P_{1/2}$-$2p^3\ ^2P^\circ_{1/2}$	−0.70	−0.71
$2s2p^2\ ^2P_{1/2}$-$2p^3\ ^2P^\circ_{3/2}$	−1.15	−1.13
$2s2p^2\ ^2P_{3/2}$-$2p^3\ ^2P^\circ_{1/2}$	−1.05	−1.05
$2s2p^2\ ^2P_{3/2}$-$2p^3\ ^2P^\circ_{3/2}$	−0.32	−0.33

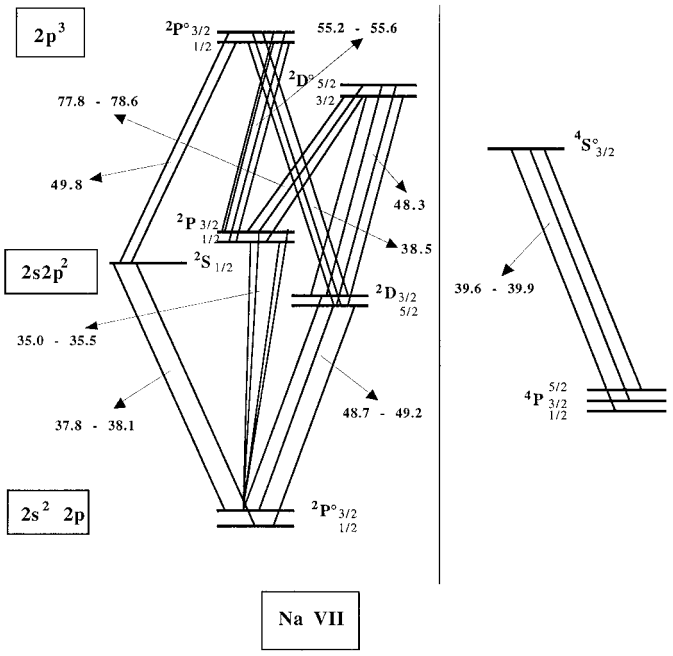

Fig. 2. Partial Grotrian diagram indicating the strongest transitions of interest for the present study. The term differences are not to scale. The transition wavelengths are given in nm.

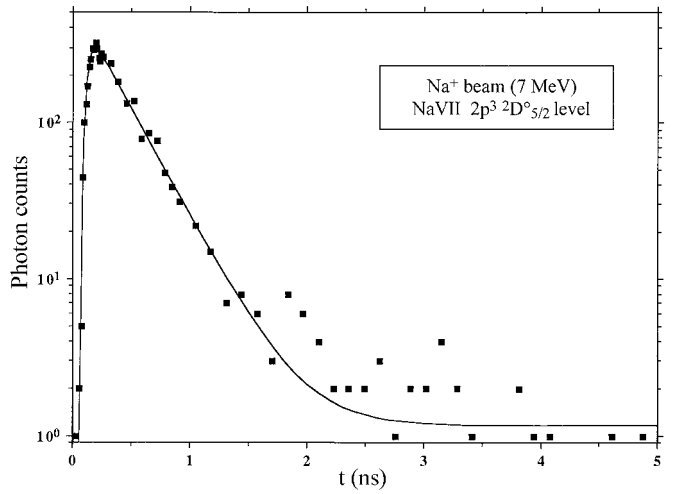

Fig. 3. Example of a beam-foil decay curve.The upper level of the transition is $2p^3\ ^2D^\circ_{5/2}$. The data have been fitted with a sum of two decaying exponentials convoluted with a Gaussian shaped observation window. The speed of the ions was 7.58 mm/ns.

number of features that are important for the interpretation of lifetime data [35–38]. One is the eigenvector composition of the $nsnp^2\ ^2S$, ^2P levels that change drastically along the isoelectronic sequence. The other is the lifetime pattern of the $nsnp^2$ and np^3 doublet levels. It is well known that multi-exponential analyses to synthetic data with noise can be ambiguous. This is because a fit procedure that optimizes the fit parameters in a quest for a minimum reduced chi-squared value moves on a hypersurface in parameter space that may have false minima or very low gradients. The undisputed systematics of the term structure and of the lifetime pattern in B-like ions (see [9,10]) make it advisable to obtain some orientation from this knowledge in the evaluation process. Without the resources for an exhaustive experimental study, we have chosen fit solutions (with near-minimum chi-squared values) that at least come close to the expected cascade pattern, in some cases using constrained fits with cascade lifetimes fixed to theoretical data and fitting only cascade amplitudes (and the primary decay amplitude and lifetime). The error estimates of our lifetime results reflect both the signal statistics and the range of variability of the fit results under such conditions.

In the B sequence, the $2s2p^2\ ^2S_{1/2}$ level lifetime is slightly larger than that of most cascades (notably from $2p^3\ ^2P^\circ$), and thus a slope of the decay curve can be expected that, after a section affected by growing-in cascades, approaches the true level lifetime. The $2s2p^2\ ^2P$ levels are somewhat shorter lived than both $2p^3\ ^2P^\circ$ and $2p^3\ ^2D^\circ$ cascades. The primary and cascade lifetimes, however, are so close to each other that multiexponential analyses are almost bound to fail. In the absence of a proper ANDC measurement [38], a cascade simulation analysis can provide a consistency check of the calculated lifetime pattern, or provide a simulated decay curve to test the multi-exponential analysis approach. It is typical that in such a case a multi-exponential analysis returns an apparent primary lifetime that exceeds the input value to the simulation by 30-50%, and the same happened with many of the fit attempts on the $2s2p^2\ ^2P$ level decay curve here when comparing to theoretical data. Because of the statistical weight, the $2s2p^2\ ^2D_{3/2,5/2}$ decays yield the strongest signal decay curves. The $2p^3\ ^2P^\circ$, $^2D^\circ$ cascades boost this intensity as growing-in cascades with lifetimes that are shorter, but within the same order of magnitude as the primary level. If only those levels contributed, it would be straightforward to extract the primary level lifetimes from the $2s2p^2\ ^2D$ decay curve after the growing-in cascades have died out. However, the yrast chain of levels (levels of maximum angular momentum l for a given principal quantum number) feeds these levels, and the yrast cascade tail has both fast and long-time components.

5.2 Doublet system of Na VII

$2p^3\ ^2P^\circ$

As no direct measurements are available for this term, the only possible comparison is with the theoretical values. The different theoretical methods give approximately the same values for $J = 1/2$ and $J = 3/2$ levels and show a scatter of 15%.

$2p^3\ ^2D^\circ$

The two fine structure levels ($J = 3/2$ and $J = 5/2$) have nearly the same theoretical lifetimes. The MCDF result are 0.271–0.272 ns which are somewhat higher than the HFR data (0.244–0.245 ns) while the experimental result agrees within the errors with theory.

$2s2p^2\ ^2S$

Two distinct measurements were performed for this lifetime ($J = 1/2$) at two different energies (4.5 and 7.0 MeV). Neglecting cascades, a single-exponential fit yields an apparent lifetime of more than 0.2 ns. However, constraining the fit of the primary decay by forcing a major cascade of the calculated lifetime of the $2p^3\ ^2P^\circ$ levels results in $2s2p^2\ ^2S_{1/2}$ level lifetime values of 0.15 and 0.16 ns that agree with each other within the 0.01 ns errors and are close to the theoretical values which scatter close to 0.16 and 0.14 ns. This rather simple case corroborates the above discussion and the application of basic atomic structure knowledge to the more complicated decay curves of the other levels studied, too.

$2s2p^2\ ^2P$

The only previous experimental measurement on Na VII has been obtained for this multiplet [7]. Although in that work the ion beam energy was too low for an observation of the Na VII spectrum under good conditions, these authors performed a lifetime measurement for the $2s2p^2\ ^2P$ term using the unresolved $2s^22p\ ^2P^\circ$-$2s2p^2\ ^2P$ transition. Their result agrees well with our MCDF calculation. With a three-exponential fit, we find a primary lifetime that agrees reasonably well with the earlier finding and with theory. The two cascade components, however, do not individually correspond to the $2p^3\ ^2P^\circ$, $^2D^\circ$ levels, but include a longer-lived cascade tail as well.

$2s2p^2\ ^2D$

The two measurements performed in the present work for the $J = 3/2$ and $J = 5/2$ values lead to nearly identical results. The two present calculations agree within 2–3% with the measurements.

5.3 Quartet system of Na VII

$2p^3\ ^4S^\circ$

The level ($J = 3/2$) has a measured lifetime of 0.095 ns (when putting in a growing-in cascade). The theoretical values (0.087 ns and 0.088 ns) are slightly lower than the experimental result.

5.4 Na VIII

Our lifetime measurement for the $2s2p\ ^1P_1^\circ$ level of Na VIII is in close agreement with the theoretical values of 0.229 (HFR) and 0.206 (MCDF) ns, respectively. This then also fits well to the isoelectronic trend as established by isoelectronic smoothing of experimental data [39,40] and to recent MCDF calculations of the sequence [41].

6 Conclusions

The beam-foil method has been used to record Na spectra in the 30-60 nm region and to measure, for the first time, the lifetimes of seven $n = 2$ levels of Na VII and Na VIII. The results are compared with calculations performed with two different approaches (HFR and MCDF). Theory is generally in very good agreement with experiment. The new theoretical results for the spin-allowed transitions are expected to be very accurate. Larger uncertainties pertain to the predictions on some of the weak intercombination lines that are extremely sensitive to the small mixings appearing in the calculations of the wavefunctions.

Financial support from the Belgian National Fund for Scientific Research (FNRS) is acknowledged. The provision of a reliable Na ion beam by the Bochum crew of operators is greatly appreciated.

References

1. W.C. Martin, R. Zalubas, J. Phys. Chem. Ref. Data **10**, 153 (1981).
2. J. Söderqvist, Nova Acta Regiae Soc. Sci. Ups., Ser. IV **9**, 1 (1934).
3. J. Söderqvist, Ark. Mat. Astron. Fys. **30**, 1 (1944).
4. B.C. Fawcett, J. Phys. B **3**, 1152 (1970).
5. B. Edlén, 1979 (unpublished material), quoted by Martin and Zalubas (1981).
6. R.L. Kelly, J. Phys. Chem. Ref. Data, Vol. **16**, Suppl. 1 (1987).
7. J.-P. Buchet, M.-C. Buchet-Poulizac, M. Druetta, Phys. Scripta **18**, 496 (1978).
8. E. Träbert, P.H. Heckmann, H. v. Buttlar, Z. Phys. A **280**, 333 (1977).
9. E. Träbert, P.H. Heckmann, W. Schlagheck, H. v. Buttlar, Phys. Scripta **21**, 27 (1980).
10. E. Träbert, G. Schneider, P.H. Heckmann, Phys. Scripta **27**, 407 (1983).
11. W.L. Wiese, M.W. Smith, B.M. Miles, *Atomic Transition Probabilities*, Vol. II, NSRDS-Nat. Bur. Stand. 22 (US Government Printing Office, Washington D.C., 1969).
12. M. Cohen, A. Dalgarno, Proc. Roy. Soc. Lond. A **280**, 258 (1964).
13. A.W. Weiss, Phys. Rev. **188**, 119 (1969).
14. D.R. Flower, H. Nussbaumer, Astron. Astrophys. **45**, 349 (1975).
15. W. Dankwort, E. Trefftz, J. Phys. B **10**, 2541 (1978).
16. B.C. Fawcett, At. Data Nucl. Data Tables **22**, 473 (1978).
17. R.D. Cowan, Phys. Rev. **163**, 54 (1967).
18. R.D. Cowan, D.C. Griffin, J. Opt. Soc. Am. **65**, 1010 (1976).
19. G.E. Bromage, *The Cowan-Zealot Suite of Computer Programmes for Atomic Structure*, Appleton Laboratory report, AL-R-3, Abingdon, Great Britain (1978).
20. A. Farrag, E. Luc-Koenig, J. Sinzelle, At. Data Nucl. Data Tables **24**, 227 (1979).
21. A. Farrag, E. Luc-Koenig, J. Sinzelle, J. Phys. B **13**, 3939 (1980).
22. R.P. McEachran, M. Cohen, J. Quant. Spectrosc. Radiat. Transfer **27**, 111 (1982).
23. C. Lavin, I. Martin, J. Quant. Spectr. Radiat. Transfer **50**, 611 (1993).
24. D. Luo, A.K. Pradhan, J. Phys. B **22**, 3377 (1989).

25. M.J. Seaton, *The Opacity Project*, compiled by the Opacity Project Team (Institute of Physics Publishing, Bristol and Philadelphia, 1995).
26. I.P. Grant, B.J. McKenzie, P.H. Norrington, D.F. Mayers, N.C. Pyper, Comput. Phys. Commun. **21**, 207 (1980).
27. B.J. McKenzie, I.P. Grant, P.H. Norrington, Comput. Phys. Commun. **21**, 233 (1980).
28. K.G. Dyall, I.P. Grant, C.T. Johnson, F.A. Parpia, E.P. Plummer, Comput. Phys. Commun. **55**, 425 (1989).
29. H.L. Zhang, D.H. Sampson, At. Data Nucl. Data Tables **56**, 41 (1994).
30. J. Granzow, P.H. Heckmann, E. Träbert, Phys. Scripta **49**, 148 (1994).
31. E. Biémont, E. H. Pinnington, J.A. Kernahan, G. Rieger, J. Phys. B: At. Mol. Opt. Phys. **30**, 2067 (1997).
32. E. Biémont, J.-F. Dutrieux, I. Martin, P. Quinet, J. Phys. B: At. Mol. Opt. Phys. **31**, 3321 (1998).
33. Z.S. Li, S. Svanberg, E. Biémont, P. Palmeri, J. Zhangui, Phys. Rev. A **57**, 3443 (1998).
34. E. Biémont, P. Quinet, Phys. Rev. Lett. **81**, 3345 (1998).
35. E.H. Pinnington, W. Ansbacher, A. Tauheed, E. Träbert, P.H. Heckmann, G. Möller, J.H. Blanke, Z. Phys. D **17**, 5 (1990).
36. J. Doerfert, E. Träbert, Phys. Scripta **47**, 524 (1993).
37. L. Engström, M. Kirm, P. Bengtsson, S.T. Maniak, L.J. Curtis, E. Träbert, J. Doerfert, J. Granzow, Phys. Scripta **52**, 516 (1995).
38. L.J. Curtis, H.G. Berry, J. Bromander, Phys. Lett. A **34**, 169 (1971).
39. N. Reistad, I. Martinson, Phys. Rev. A **34**, 2632 (1986).
40. E. Träbert, Z. Phys. D **9**, 143 (1988).
41. P. Jönsson, C. Froese Fischer, E. Träbert, J. Phys. B: At. Mol. Opt. Phys. **31**, 3497 (1998).
42. O. Sinanoglu, Nucl. Inst. Meth. **110**, 193 (1973).